DOI: 10.2478/sspjce-2025-0008

Polymer Based Shear Connectors for Composite Structures

Michala Weissova[1*], Vincent Kvocak[1], Daniel Dubecky[2], Lukas Kapolka[1]

[1]Technical University of Kosice, Faculty of Civil Engineering, Institute of Structural Engineering and Transportation Structures, 040 01 Kosice, Slovakia
[2]Technical University of Košice, Faculty of Civil Engineering, Center for Research and Innovation in Construction, Park Komenského 10A, 042 00 Košice, Slovakia
[*]e-mail: michala.weissova@tuke.sk

Abstract

This work examines the performance of glass-fiber-reinforced polymer (GFRP) shear connectors within concrete composite beams with attention to their mechanics and wider applications for sustainable structures. Beyond comparing two different connector geometries, the work broadens to cover their suitability for cyclical loading, long-term deflection, and structural fatigue exposure. By drawing on both experimental push-out testing and numerical simulation using the finite element method (FEM), the research provides a rich picture of GFRP-based joint mechanics. The analysis further delineates recommendations for long-term use of GFRP members of civil applications with a focus on design optimization, benefit-cost ratios, and resistance to corrosion. These findings form the basis for next generation building material aimed at lowering maintenance costs and carbon impacts.

Keywords: push-out assessment, experimental analysis, GFRP, FEM analysis

1 Introduction

Construction material innovations are ever more influenced by the necessity for corrosion resistance and increased structural durability that is encompassed by the performance expectations of modern times for traditional materials like steel and concrete structures. Fiber-reinforced polymers (FRPs) or glass fiber reinforced polymer (GFRP) present a compelling mechanical performance along with long durability that promises much for their application in various structural configurations. This paper examines the mechanical performance and simulation-based modeling of GFRP shear connectors, which are a key element to ensure efficient composite, concrete and prefabricated members perform as desired under a load. The experimental work employs the modified push-out assessment for determining the strength of bond and failure modes under cyclic loading. At the same time, a computer-based model is simulated on Abaqus/CAE, which is the same condition to observe stress distribution, material response, and forecast long-term performance. The goal is to evaluate GFRP structural reliability and outline guidelines for its application in civil structures like pedestrian bridges, noise barriers, and precast concrete schemes.
Composite materials are a part of the market that is taking the place of widely used material nowadays. As a result of the rapid advancement of science and technology, industry, and

technology, material requirements for modern use are becoming increasingly stringent. The traditional construction material currently used slowly no longer satisfies the needs of modern technology. Thus, higher strength properties and higher resistance to external factors are taking center stage with commodity materials that are composite materials. As a result of the step-by-step growth of demand for strength and resistance, which cannot be accomplished effectively with the methods of present times, such as additives, heat treatment, or forming, the evolution of composite materials has become a necessity. Mainly because of that, various types of material began to be brought together to be processed as single building material, a composite material, with the goal of integrating the favorable properties of the individual material [1,2,3].
For strengthening, the fibers are aligned in a specific direction uniformly. The fibers may either be metallic or non-metallic. Steel fibers are some examples of metallic fibers, whose strength is enhanced with increased plastic deformation, and tungsten and molybdenum fibers. Carbon fibers are some examples of non-metallic fibers, which possess a large modulus of elasticity, strength limit, good thermal resistance, and light weight.
Glass fibers are also a class of non-metallic fibers that are of low weight and thermal conductivity but high chemical and thermal stability with enough strength. Among glass fibers, two basic forms are manufactured: continuous and staple forms. Continuous form is prepared by drawing fibers from hot glass mass, and staple form is prepared by drawing glass fibers from a flow of hot glass and cutting them to the desired length. Boron, ceramic, and whisker fibers are other forms of fibers [4].

1.1 Manufacturing of composite materials

The value of the composite material is that it unifies the properties of the fibers (carbon, boron, tungsten, glass, etc.) with resin (polymer) to produce a material that possesses the mechanical properties of a material based on mineral resources.
Many different technologies and ways are used to create composite materials. To obtain the required quality and a high content of mechanical and physical properties, a proper technology and method of preparation should be selected. Technologies and processes for production are made suitable for laboratory and industrial applications.
Technologies to produce composite materials include:

- Pultrusion – production by pulling (open or closed profiles, rods, sheets)
- Filament winding (circular tubes)
- Molding (walkway gratings)
- Hand lay-up (components of covers and lids)
- SMC – Sheet Molding Compound – sheet pressing (manhole covers)
- Pressing
- Injection molding
- Extrusion
- Liquid resin transfer
- Pressure rolling

Composite material manufacturing using the technology of pultrusion involves pulling the material through a preheated steel mold with a pulling tool. It is a continuous manufacturing method of reinforced resins of different shapes and dimensions with the input material being a blend of liquid resin and reinforcing fibers. Pultrusion technology provides a higher volume fraction of fibers within the resulting profile. Compared to hand laying with about 20% content of fibers and compressions molding with 40% content, profiles made using pultrusion have over 70% of the content as fibers. The material travels through the production line at a rate of up to 30 to 150 cm per minute. The manufacturing process produces a solid profile with a wall of at least 1.5 mm thickness.

2 Experimental analysis

For assessment of mechanical performance of shear connectors made of GFRP, a tailored push-out test setup based on a modified protocol of EN 1994-1-1 was used [5]. Authors cast concrete around composite GFRP members using ridged and perforated strip variants to evaluate the quality of the bond. Advanced methods for placement ensure separation of connector-concrete interaction, for example, using polystyrene barriers. Test sequences comprised controlled loading to 40% of failure point, followed by repeated unloading sequences, simulating dynamic stress exposure to the actual environment. Measurement concentrated on slip response and load-carrying capacity before failure onset.

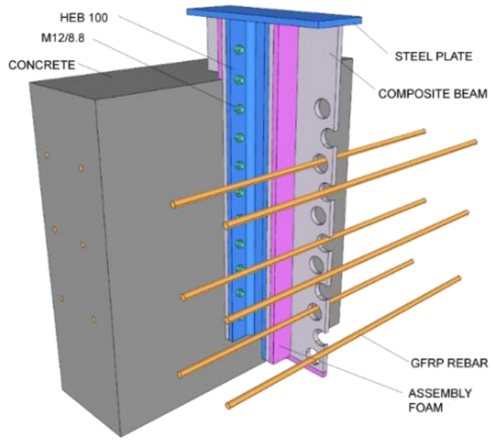

Fig. 1. Composition of experimental specimen

The primary principle of the push-out assessment is to determine the shear resistance of the continuous strip. The push-out specimen consists of two concrete blocks, each measuring 200 mm in width, 600 mm in length, and 600 mm in height. Continuous connectors with a bonding length of 400 mm were embedded into these concrete blocks. The composite connectors are made from two beams cut with a water jet from a composite profile 600 mm in length, embedded such that their position was 100 mm from the bottom edge of the block and extended 100 mm above the top edge. To determine the actual bond resistance and prevent the beam from being pressed into the concrete, a 10 mm-thick polystyrene sheet was placed beneath the beam [1].

The standard test specifies the dimensions of the specimen as well as the loading procedure. Loading begins with a gradual application up to 40% of the expected failure load, followed by 25 loading-unloading cycles between 5% and 40% of the failure load. After the cyclic phase, the specimen is loaded steadily until failure.

Failure should not occur within the first 15 minutes of sustained loading. If it does, it suggests the loading rate was too rapid, leading to inaccurate results that don't reflect real-world conditions. The longitudinal slip should be measured continuously during the test or at least up to 80% of the maximum expected load. The arrangement of the tested specimen is shown in Figure 2.

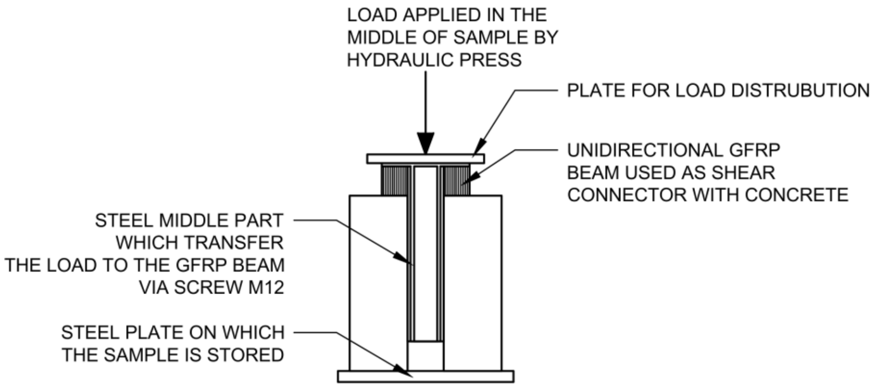

Fig. 2. Boundary conditions while assessment in process

Two forms of the composite connectors that the authors chose for experimental validation of the bond are presented in Fig. 3. The first form consisted of a 57 mm comb height ridge strip. A 10 mm GFRP reinforcement bar was placed inside each wave. The second form was a perforated strip with a diameter of 32 mm with GFRP reinforcement [6,7].

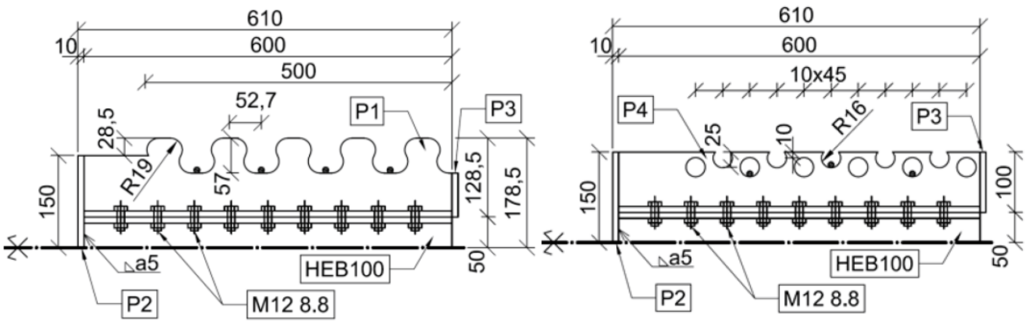

Fig. 3. Types of used continuous shear connectors in experimental analysis: a) ridged strip (HP), b) perforated strip (PP)

2.1 Material characteristics

According to the experimental determination of material properties, material properties have been listed in Table 1. These properties play an important role in determining the progression of experiments. Without them, proper analysis using the finite element method is impossible to do [4].

Table 1. Material characteristics of GFRP beam material in both fiber orientations

Name of value	Direction	Unit	Value
Tensile strength, σ	∥	MPa	451.0934
	⊥	MPa	53.4883
Young modulus, E	∥	GPa	35.1538
	⊥	GPa	7.1016
Elastic strain, ε_{el}	∥	-	0.0086
	⊥	-	0.0091
Plastic strain, ε_{pl}	∥	-	0.0078
	⊥	-	0.0077
Shear strength, τ	∥	MPa	56.3653
	⊥	MPa	19.4751
Shear modulus, G	∥	GPa	3.3349
	⊥	GPa	1.4749
Shear strain, γ	∥	-	0.0093
	⊥	-	0.0093

Methods for assessment, and outcomes of concrete strength verification based on concrete age, have been performed experimentally using the methods presented in the Standards specifying concrete material properties. From the presented experiments as per EN 1992-1-1 [8], material properties of the concrete have been calculated from the table provided there, Table 2. As per the norm, from the transverse tensile strength of the concrete, the axial tensile strength is calculated as 0.9 times that strength. From the experiments presented 28 days after specimen casting, Table 2 presents the outcomes of the measured parameters. As a comparison, the table moreover presents the standard values of the measured properties [2].

Table 2. Material characteristics of concrete C30/37

Name	Unit	Value from lab	Standard value
f_{ck}	MPa	31.427	30.0
$f_{ck,cube}$	MPa	39.814	37.0
f_{cm}	MPa	39.427	38.0
f_{fl}	MPa	4.807	4.5
$f_{ct,sp}$	MPa	2.782	3.2
f_{ct}	MPa	2.504	2.9
f_{ctm}	MPa	2.504	2.9
$f_{ctk.0.05}$	MPa	1.752	2.0
$f_{ctk,0.95}$	MPa	3.255	3.8
E_{cm}	GPa	32.677	33.0
ε_{c1}	‰	2.187	2.2
ε_{cu1}	‰	3.500	3.5

3 Experimental analysis of push-out assessment

The beams were attached to a steel profile to allow for the movement of the whole central component along with the composite beams, ensuring there is enough stiffness at the joints. The authors tend to make the joint themselves, but with the involvement of the bonding of a composite beam, it was carried out with bolts. A total length of 600 mm of a central component was thus produced, where the flanges of two composite beams were attached to the steel beam flanges using steel bolts. To avoid the over-bonding of the bolts with concrete, a mounting foam was used to encase the area around the bolts. The concrete was reinforced with GFRP reinforcement to ensure that the reinforcing bars were part of the continuous strip.

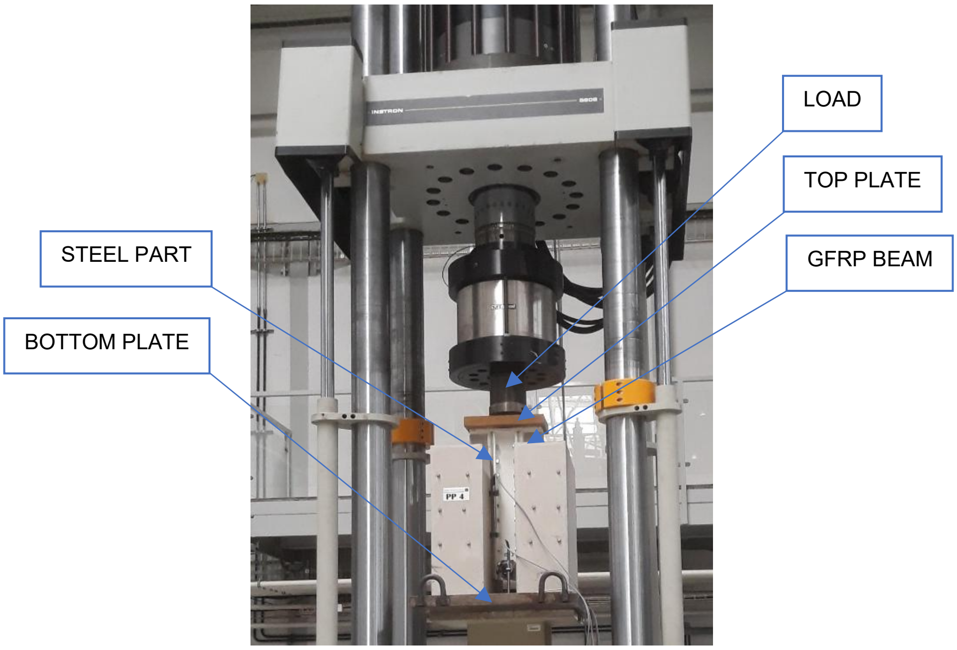

Fig. 4. Composition of experimental assessment

Loading of the specimen was done systematically within loading cycles with the specimen being loaded to 40% of expected resistance while being subsequently unloaded to 5% resistance. This was followed by 25 cycles with a minimum of 5% and a maximum of 40% of the expected resistance.

The amplitude represents the loading process during assessment of the specimen based on the steps in the standard for assessment being used. The initial steps that involve cyclic loading ensure that the relationship between the concrete and GFRP beam is correct and consistent.

The experimental verification results for the push-out evaluation are shown graphically by the resulting graphs for the continuous perforated composite connectors and for the continuous ridged connectors. The graphs show the relationship between force and displacement. The curves depict the result for each evaluated specimen, and a mean curve was calculated from the results at each loading step. The curves were calculated from listed results at the same steps of loading. At each step, average values were calculated, which allowed for the creation of the average curve.

From the graphs, the plastic deformation of composite material up to failure can be concluded. Specimen failure occurred at the area where glass fibers were cut to form the continuous shear connector.

Fig. 5. Type of damages of specimens

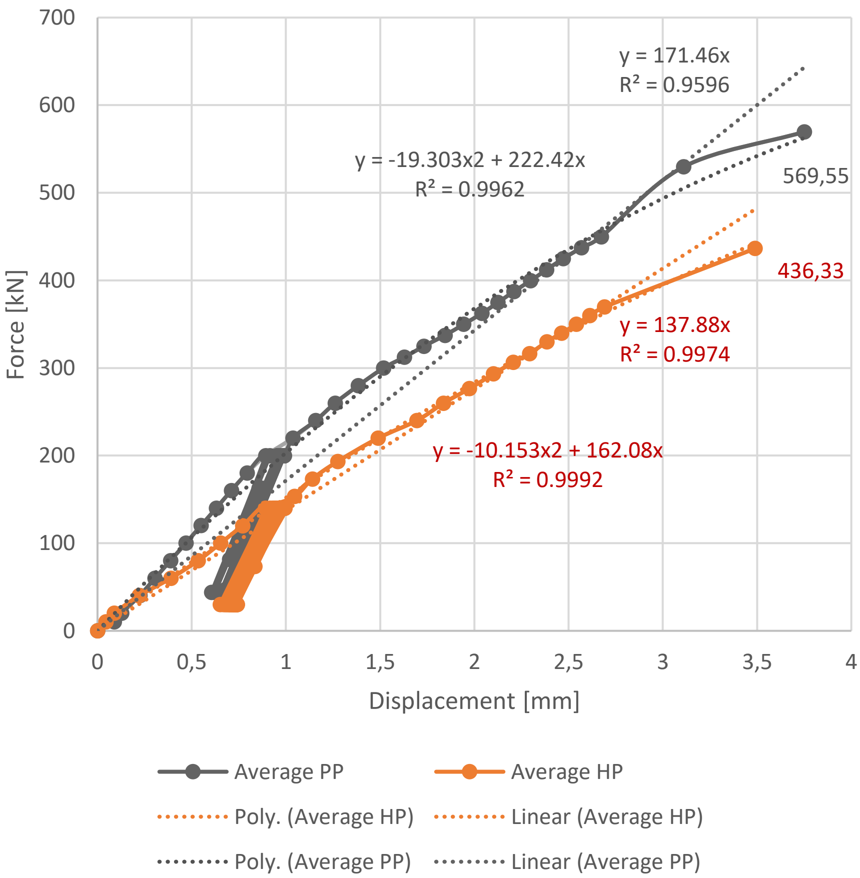

Fig. 6. Force-displacement diagram

From these experiments, one may calculate the maximum force, which is the resistance of this form of bonding at maximum deformation. The former graphs on Fig. 6 also suggest that composite materials respond elastically up to failure with minimal evidence of plasticity. The experiments showed that no surface failure of the concrete happened before the bond failed. Concrete failure took place at the top edge and bottom after being impacted, with a shape resembling a loading cone. These graphs and experimental validation suggest that the resistance of bonding with the comb strip is 436.33 kN, and, with the use of the perforated strip, is 569.55 kN.

4 FEM analysis

Finite element simulations the authors performed using Abaqus/CAE to mimic the experimental push-out tests. GFRP and concrete material response was defined using orthotropic and concrete damage plasticity models for the two, respectively. Rigid-body constraints and frictional interface boundary conditions were implemented with calibration to experimental slip-load curves. A hex-dominant element mesh was used to reduce computation error, and stress distribution outputs were validated using empirical failure modes. The model exhibited good agreement with assessment results, particularly initial stiffness and ultimate strength ranges for both connector types.
For simulating push-out test, four parts of the specimen were modelled, as shown in Figure 7. It was the concrete part wherein the GFRP beam component with shear connector, the middle steel component that is attached with GFRP beam and rebars.

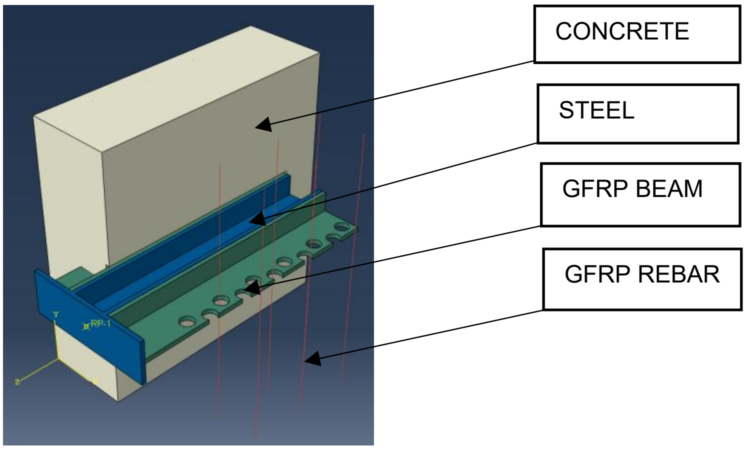

Fig. 7. The components of specimen used in Abaqus

4.1 Materials definitions

This beam is anisotropic along two directions, so it is an orthotropic material where material properties should be defined for all directions. Proper definition was carried out using an elastoplastic analysis. It is necessary to input material density for each material for a 3D FEA analysis. Tensile and shear modulus measured values were used by the authors to define the material's elastic properties. As the measured value of Poisson's ratio was not provided, a value

of 0.33 has been used. The input is defined by the software manual using 'Engineering Constants' (Table 3).
In order to define plastic behaviour of an anisotropic composite material, 'Plastic' module with 'Potential' module was used. It follows a function named 'Hill's potential function' (Table 4, Table 5) [9].
The material properties of concrete the authors determined from laboratory experiments which are presented in Tab. 1 and Tab. 2. The ‘Concrete Damage Plasticity' method was used to determine concrete properties. This method is based on defining the material properties of concrete with modules offered by this method, that is, 'Plasticity,' 'Compressive Behavior,' and 'Tensile Behavior' [10,11].

Table 1: Material properties of concrete used in model

Concrete				
Density		Elastic		
Mass density (t/mm^3)		Young's modulus (MPa)	Poisson's ratio	
2.29E-09		32677	0.2	
Plastic				
Plasticity				
Dilation Angle (°)	Eccentricity	f_{b0}/f_{c0}	K	Viscosity Parameter
31	0.1	1.16	0.67	0.0005
Compressive Behavior		Concrete Compression Damage		
Yield Stress (MPa)	Inelastic strain	Damage parameter	Inelastic Strain	
12.57080	0.00000	0.00000	0.00000	
26.71295	0.00085	0.00000	0.00085	
31.42700	0.00169	0.00000	0.00169	
17.28485	0.00316	0.45000	0.00316	
12.57080	0.00339	0.60000	0.00339	
Tensile Behavior		Concrete Tension Damage		
Yield Stress (MPa)	Cracking Strain	Damage parameter	Cracking Strain	
2.09132	0.00000	0.00000	0.00000	
1.39422	0.00015	0.33333	0.00015	
0.78426	0.00035	0.62500	0.00035	
0.34855	0.00066	0.83333	0.00066	

Table 2: Material properties of GFRP beam used in model

GFRP beam		
Density		
Mass density (t/mm^3)		
1.8E-09		
Elastic - Engineering constants		
E_1 (MPa)	*E_2 (MPa)*	*E_3 (MPa)*
35676	7102	7102
ν12	ν13	ν23
0.33	0.33	0.33
G_{12} (MPa)	*G_{13} (MPa)*	*G_{23} (MPa)*
3335	3335	1475
Plastic		
Yield Stress (MPa)	Plastic strain	
263	0	
451	0.01248	
Potential		
R_{11}	R_{22}	R_{33}
1	0.11917	0.11752
R_{12}	R_{13}	R_{23}
0.072969	0.072969	0.21891

Table 3: Material properties of GFRP rebar and steel used in model

GFRP rebars		**Steel**	
Density		Density	
Mass density (t/mm3)		Mass density (t/mm3)	
1.8E-09		7.85E-09	
Elastic		Elastic	
Young's modulus (MPa)	Poisson's ratio	Young's modulus (MPa)	Poisson's ration
50000	0.33	210000	0.3

4.2 Boundary conditions

Contact between individual components was established to generate friction between the concrete and the composite strip with a friction coefficient of 0.18. To get better element convergence and proper definition of contacts, the 'Penalty Contact Method' has been used that involves master and slave surface designations. Because concrete is of a larger representation within the overall model, the master surfaces are concrete surfaces, and the slave surfaces are the composite surfaces (Figure 8-left).

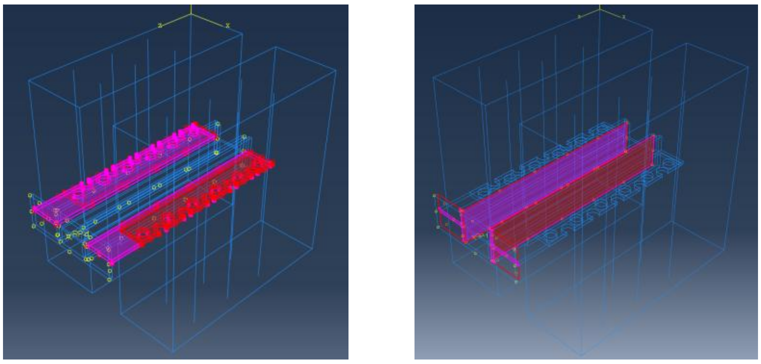

Fig. 8. Contact components (concrete-GFRP, GFRP-steel)

A perfectly rigid interface was established between the steel and the composite, which was fastened using bolts. Definition of the master and slave surfaces was also required for this purpose, with the steel surfaces being designated master and the composite surfaces slave. Another necessary setup for this module is the stiffness of the loading surface. The 'Rigid Body' option was used for this attribute so that the surface is not deformed while loading.

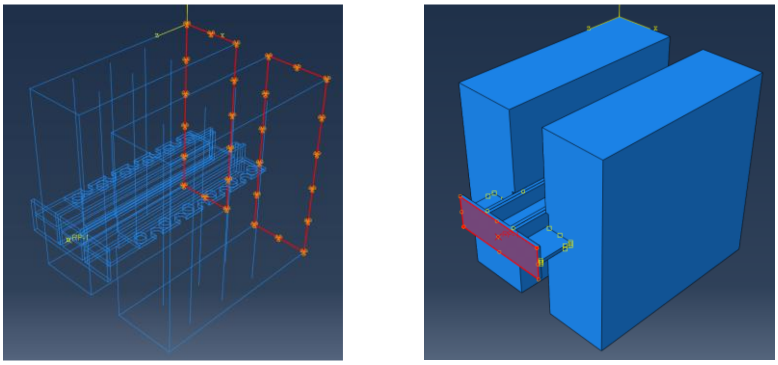

Fig. 9. Boundary conditions

Boundary conditions were imposed to avoid vertical concrete displacement (Fig. 9-right). The arrangement was done before loading the specimen. The load came from the vertical direction based on the loading cycle of each assessment of the composite strip.

4.3 Mesh definition

Another key to valuable FEM calculations is proper mesh setup. A hexagonal 3D mesh was desired for the FEM analysis of the push-out evaluation, which has the basic benefit of eliminating incorrect elements and accelerating the computation. As a result of the intricate geometry of push-out evaluation elements, parts needed to be split into basic elements to form the hexagonal 3D mesh. This splitting only influences the elements and the whole component.

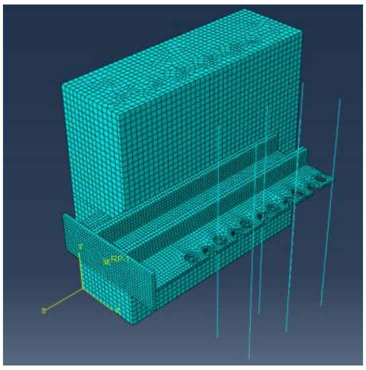

Fig. 10. The example of mesh for the specimen for push out assessment

For the perforated strip, 140,675 elements, 165,017 nodes, and 495,054 variables were generated for analysis, as well as all inputs provided in the preceding modules.
For the ridged strip, there were 130,612 elements, 157,167 nodes, and 471,504 variables generated for the analysis.

4.4 Results of FEM analysis

Below are resulting plots and stress distributions for individual specimens plotted alongside the average experimental results. Increasing processor usage to 100% and the number of logical processors to 20 sped up the analysis, cutting the computation time by an estimated 2–3 times. The overall computation time was 1,150 seconds, or roughly 19.2 minutes.

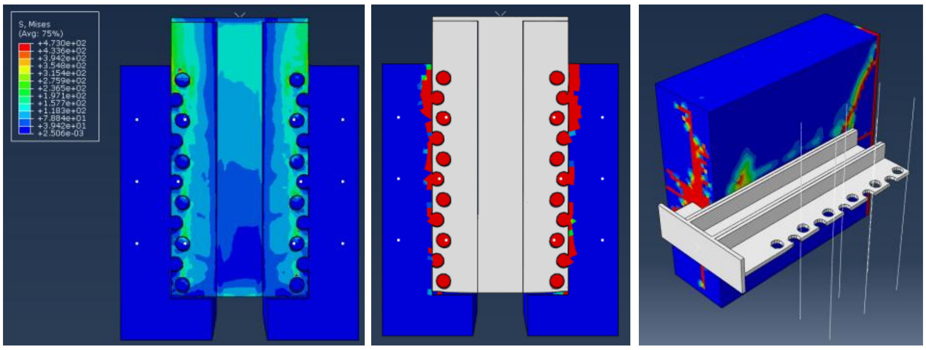

Fig. 11. The results from FEM analysis for perforated continuous shear connector (Von Mises stress, concrete-compress, concrete-tensile)

After the experimental testing for verification of the numerical model, stress values for the bonded parts can be calculated with higher accuracy. Fig. 11 illustrates the distribution of stress within the specimen, along with the compressive and tensile failure of the concrete. The accuracy of the model comparison is presented in Figure 12, which also indicates a small difference due to material properties incorporated into the model that could not be exactly established experimentally.

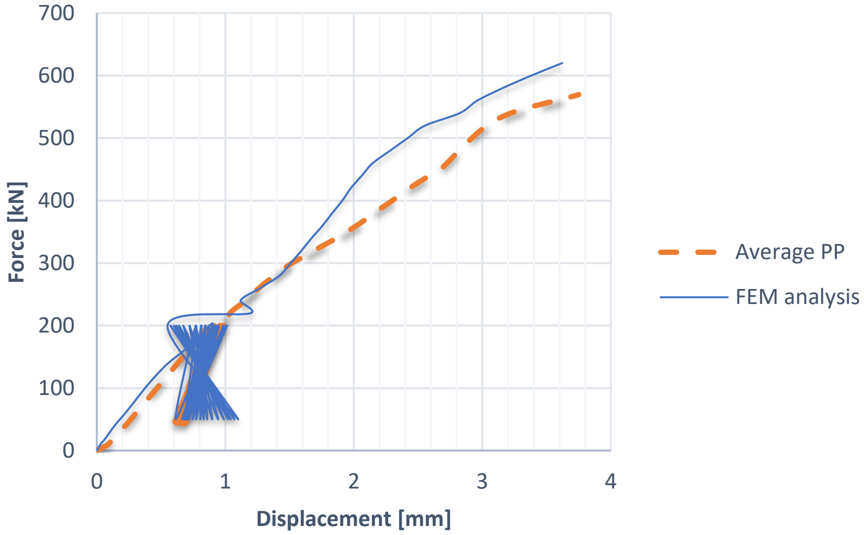

Fig. 12. The comparison of results from FEM and experimental analysis for perforated continuous shear connector

For the ridged strip, the analysis took a total of 1.147 seconds, which is approximately 19.1 minutes.

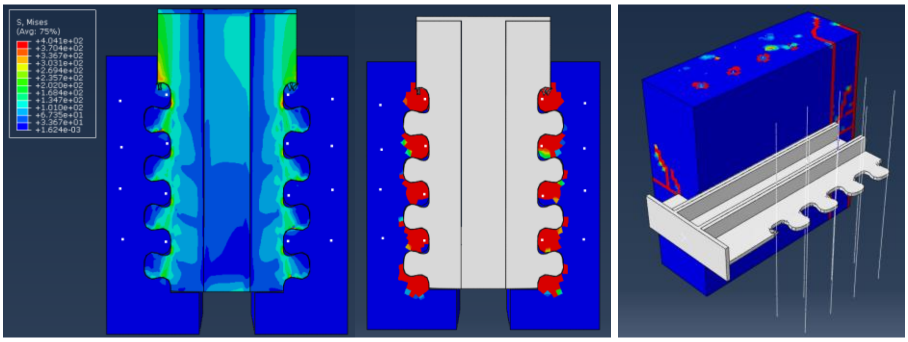

Fig. 13. The results from FEM analysis, for ridges continuous shear connector (Von Mises stress, concrete-compress, concrete-tensil)

Both of these results are derived from the numerical simulation of the comb strip type of bonding element. They are presented in Fig. 13. As with the case for a perforated strip bonding element, comparison between the experiment and the numerical model is depicted in Figure 14.

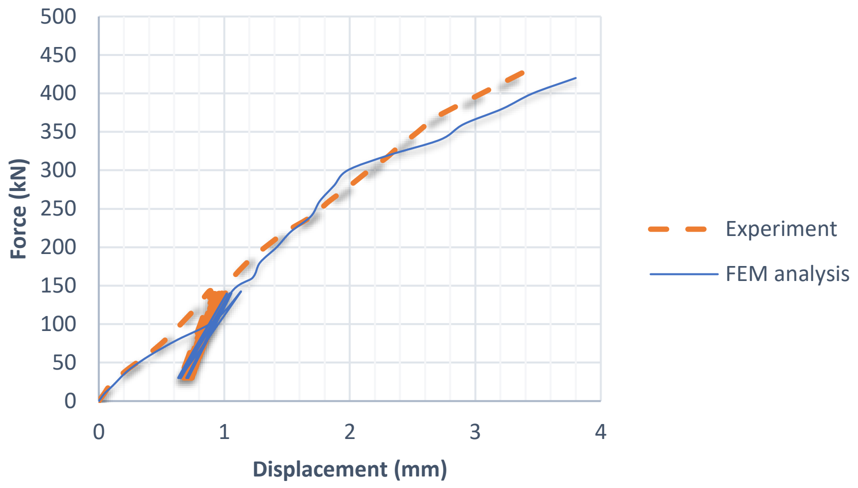

Fig. 14. The comparison of results from FEM and experimental analysis for ridged continuous shear connector

From the comparison with the experimental analysis, FEA indicates the same results as the experimental results, and thus FEA may be a suitable alternative to experimental analysis when conducting future similar analyses. Aside from the comparison of the deformations, it could be said that stress distribution within the composite and concrete as per FEA approximates the actual experimental trend. Component from the stress results, there is a clear indication that concrete pieces failed at the places where the failures were anticipated based on the actual experiment.

5 Conclusion

This research validates the feasibility of shear connectors based on GFRP as lightweight, corrosion-proof steel alternatives for composite structures. Numerical and experimental findings emphasize clear benefits from an elastic perspective and manufacturability, although at the expense of their ultimate strengths. Critical applications, such as bridge applications, require further evaluation for fatigue, cycle durability, and long-term adhesive bonding. This work, however, provides a basis for the implementation of advanced polymer composites in structural joints.

According to these findings, it is possible to establish that the resistance of the ridged strip is roughly 30% lower, which has a major impact on matrix failure during the test. The resistance of the perforated strip is roughly 20% lower than that of steel.

Given the benefits of composites, e.g., corrosion resistance and low material weight, the composite beam may be seen to qualify as an adequate bonding element. However, for applications of these beams to be applied to bridge constructions, experimental validation of the dynamic, fatigue, bending, and long-term loading on this form of bonding is required. Furthermore, the implementation of hybrid assessment methodologies and extensive numerical sensitivity analyses for this research indicate that variations of connector geometry greatly affect efficiency of the bond, especially under low-cycle fatigue regimes. Environmental

exposure scenarios, e.g., freeze-thaw cycling and chloride penetration, could be implemented in subsequent studies to ensure long-term usage of the material. With advancements in composite technology, the integration of sensor-based health monitoring with GFRP components could provide for proactive maintenance needs for critical infrastructure. This presents a new frontier for integrating smart material with structural resiliency goals.
The synergy of thorough experimental characterization and validated finite element analysis provided herein highlights its potential utility with respect to present-day structural engineering challenges. These findings not only have pragmatic design consequences, but they also propose sound methodological paradigms for assessing sophisticated materials for demanding load-carrying applications.

Acknowledgement

The presented paper was supported by the project: APVV-23-0204 "Utilization of composites based on FRP for composite bridge structures" of the Slovak Research and Development Agency of the Ministry of Education, Research, Development and Youth of the Slovak Republic.
The presented paper was supported by the project: VEGA 1/0642/24 "Analysis of Composite Structural Elements Based on Composite Materials and Concrete" of the Scientific Grant Agency of the Ministry of Education Science Research and Sport of the Slovak Republic.

References

[1] Weissova, M., Kvočák, V., Dubecký, D., & Vaňová, P. (2023). The usage of polymer-based materials in civil engineering. In *IABSE Congress, New Delhi 2023: Engineering for Sustainable Development* (pp. 1080–1086). Zürich: IABSE. https://doi.org/10.2749/newdelhi.2023.1080.

[2] Sojka, J., & Váňová, P. (2012). *Fundamentals of Progressive Construction Materials*. (in Czech).

[3] Rajak, D. K., Pagar, D. D., Menezes, P. L., & Linul, E. (2019). Fiber-reinforced polymer composites: Manufacturing, properties, and applications. *Polymers*, 11(10), nestránkované. https://doi.org/10.3390/polym11101667.

[4] Ehrenstein, G. W. (2009). *Polymer Composite Materials* (1st ed.). Praha: Nakladatelství Scientia.

[5] EN 1994-1. Eurocode 4 - design of composite steel and concrete structures - Part 1: General rules and rules for buildings. 2009.

[6] Weissova, M., Kvocak, V., Dubecky, D., & Vaňová, P. (2022). Numerical analysis of shear resistance on composite beams. *IOP Conference Series: Materials Science and Engineering*, 1252(1), 012035.

[7] Weissova, M., Dubecky, D., & Kvocak, V. (2021). Experimental analysis of shear connection effect composite beams with concrete. *IOP Conference Series: Materials Science and Engineering*, 1209(1), 012067.

[8] EN 1992-1-1. Eurocode 2: Design of concrete structures - Part 1-1: General rules and rules for buildings. 2004.

[9] Vrbka, J. (2008). *Mechanics of Composite Materials*. (in Slovak).

[10] Allam, S. M., Shoukry, M. S., Rashad, G. E. & Hassan, A. S. (2013). Evaluation of tension stiffening effect on the crack width calculation of flexural RC members. *Alexandria Engineering Journal.* 52, 163–173. https://doi.org/10.1016/j.aej.2012.12.005.

[11] Hafezolghorani, M., Hejazi, F., Vaghei, R., Jaafar, M. S. B. & Karimzade, K. (2017). Simplified damage plasticity model for concrete. *Structural Engineering International,* 27, 68–78. https://doi.org/10.2749/101686616X1081